SAFETY EVALUATION BY THE OFFICE OF NUCLEAR REACTOR REGULATION

FACILITY OPERATING LICENSE NO. NPF-4
VIRGINIA ELECTRIC AND POWER COMPANY
OLD DOMINION ELECTRIC COOPERATIVE
NORTH ANNA POWER STATION, UNIT NO. 1
DOCKET NO. 50-338

1 INTRODUCTION

On Wednesday, July 15, 1987, Unit 1 of the North Anna Power Station experienced a tube rupture in steam generator C, of tube R9-C51 at the top of the seventh support plate in the cold leg. This incident occurred after the reactor had returned to 100% power following the Spring 1987 refueling outage. The operators at the plant were able to bring the reactor to a cold shutdown mode without further damage to the plant or any significant radiation release to the environment.

By letter dated September 15, 1987 (Reference 1), Virginia Electric and Power Company (the licensee) provided the document, "North Anna Unit 1 July 15, 1987 Steam Generator Tube Rupture Event Report" (Reference 2) describing its plan of action for returning the plant to full power operation. Also provided for our review was the Westinghouse Electric Corp. Report, "North Anna 1 S/G Tube Rupture and Remedial Actions Technical Evaluation" (Reference 3).

This Safety Evaluation Report presents the staff's evaluation of the adequacy of the licensee's identification of the major causal factors leading to this event and the adequacy of diagnostic and corrective measures implemented by the licensee to prevent a similar failure in the future. The staff's review was assisted by expert consultants from Oak Ridge National Laboratory in the field of eddy current testing; from Argonne National Laboratory in the field of flow-induced vibration, and from the Massachusetts Institute of Technology in the field of fatigue and fracture.

Section 2 of this SER provides a brief background of steam generator experience at North Anna prior to the rupture of tube R9-C51. The extensive steam generator inspection program conducted subsequent to the rupture event is discussed in Section 3. Section 4 details the comprehensive investigations and analyses conducted to establish the root causes of the rupture. Corrective actions implemented by the licensee to prevent a recurrence of the failure mechanism are discussed in Section 5. Staff findings and conclusions pertaining to the adequacy of the licensee's program to identify causes of the rupture event and of the diagnostic and corrective measures taken to prevent a recurrence of the event are presented in Sections 6 and 7, respectively.

2 S/G EXPERIENCE PRIOR TO THE TUBE RUPTURE

The North Anna steam generators are Westinghouse Model 51. These generators have 3388 tubes, each with an outside diameter of 0.875 inch and a wall thickness of 0.050 inch. The tubing material is Inconel 600 in the mill annealed condition. The tube support plates are carbon steel with drilled tube holes.

Since initial plant startup in 1978, North Anna Unit 1 has utilized an All Volatile Treatment (AVT) control of the secondary water chemistry. The unit experienced an inadvertent intrusion of powdex resin into the steam generators during the first operating cycle. During the intrusion event, the resin decomposed to form sulfuric acid resulting in reduced pH and increased cation activity.

A corrosion phenomenon known as "denting" as first observed at North Anna Unit 1 during the first refueling outage in 1979. "Denting" refers to the squeezing of tubes at tube-to-support plate intersections caused by a buildup of an iron oxide corrosion product (called magnetite) in the annulus between the tube and support plate as a result of corrosion of the carbon steel suppor plates.

A boric acid treatment was commenced in 1980 with the intention of arresting the progression of denting. From the time it was first observed in 1979, denting at North Anna 1 has been considered to be relatively minor in terms of the amount of diameter reduction induced at the tube to support plate intersections

(compared to what has been observed at other plants). In addition, eddy current inspections indicate that the progression of denting has been arrested since at least 1984.

Tube deformation accompanying denting leads to high tensile stresses at the surface of the tube. The most usual consequence of these high tensile streses is stress corrosion cracking (SCC). These cracks generally have an axial orientation. Although the progression of denting has been arrested since at least 1984, the potential for SCC has continued to exist since the high tensile stresses associated with denting continue to be present. Since 1985, hundreds of tubes have been plugged as a result of eddy current indications and/or leaks resulting from SCC at dented locations.

Apart from SCC, there are other potential consequences of denting which are now believed (after extensive failure analyses) to have created the conditions necessary for the rupture of tube R9-C51. This is discussed in detail in Section 4.

In addition to denting and SCC associated with denting, North Anna has also experienced non-denting-related SCC in the small radius, inner row U-bends and in the tube expansion transition region at the top of the tubesheet. Like the denting-related SCC flaws, the non-denting-related SCC flaws have been observed at numerous other plants besides North Anna Unit 1. The U-bend SCC cracks are attributable to high residual stresses in the U-bends caused by the original tube bending process during fabrication. The cracks in the expansion transition region near the top of the tubesheet are the result of the high residual stresses associated with the abrupt change in tube diameter formed when the tubes were explosively expanded against the tubesheet during S/G fabrication.

North Anna Unit 1 has also recently begun to experience wear degradation as a result of the tubes interacting against the antivibration bar (AVB) supports in the U-bend region of the tube bundle. To date, the wear degradation, as indicated by eddy current test results, has been well within the Technical Specification plugging limits.

Prior to the rupture event on July 15, 1987, the North Anna Unit 1 steam generators had most recently been inspected during the Spring 1987 refueling outage. The plant did not restart from this outage until June 29, 1987, and did not reach 100% power until July 14, 1987, the day before the event.

The Spring 1987 inspection had included a 100% inspection of the population of unplugged tubes in each steam generator. As a minimum, all tubes were inspected from the hot leg tube end to the seventh (i.e., uppermost) support plate on the hot leg side. However, some tubes were inspected around the U-bends including some tubes which were inspected over their full length. In steam generator C (which contained the tube which subsequently ruptured), 24% of the tubes were inspected around the U-bend to at least the seventh support plate on the cold leg side; 16% of the tubes in steam generator C were inspected over their full length. This inspection program exceeded minimum plant Technical Specification requirements.

Tube R9-C51 in S/G C, which subsequently ruptured, had been inspected from the hot leg end to the seventh support plate on the hot leg side during the Spring 1987 outage, but had not been inspected at the seventh support on the cold leg side where the rupture occurred. Indeed, a review of past records indicates that this particular location had not been inspected since 1980. As will be explained later in this report, the failure mechanism associated with the rupture involves rapid crack propagation (i.e., no more than a few days) from the point of initiation to rupture. It is not clear that even if the upper support plate location on the cold leg side had been inspected during the Spring 1987 outage, that a detectable indication would have been present.

A total of 263 tubes were plugged during the Spring 1987 outage. Most of these were the result of SCC indications at dented support plate indications. Numerous other tubes were plugged as a result of SCC indications at the expansion transition location of the tubes near the top of the tubesheet.

3 POST-EVENT INSPECTION PROGRAM

Subsequent to the rupture event, the identity of the ruptured tube (i.e., R9-C51) was determined by observing leakage from the filled secondary side into the

drained primary side. This was followed by an eddy current examination of the tube to identify the failure location. A fiber optic-video device was then inserted to permit visual examination of the failure location. The failure was observed to involve a complete (360°) circumferential fracture of the tube at the upper edge of the seventh (uppermost) support plate on the cold leg side.

A portion of the ruptured tube on the cold leg side up to and including the fracture surface was removed from the steam generator for detailed examination. The results of these examinations and the determination of the tube failure mechanism are described in Section 4 of this report. In parallel with the assessment of the failure mechanism, the licensee commenced a comprehensive eddy current inspection program of all three steam generators as described in Section 3.1 below.

3.1 Eddy Current Inspection Scope and Methodology

The eddy current test (ECT) inspection program consisted of three major elements. First, all portions of tubes not inspected during the Spring 1987 outage were inspected with a bobbin coil probe (with coils coaxial to the tube), which is the industry standard. (As noted earlier, the fracture location on tube R9-C51 had not been inspected during the Spring 1987 outage.) Second, all tubes were inspected to the seventh (uppermost) support plate on both the hot leg and cold leg sides using a "pancake array" (8 x 1) probe. This probe consists of an overlapping array of 8 independent pancake coils spring loaded against the inner surface of the tube. This probe is more sensitive to circumferential flaws (such as those associated with the rupture) than the standard bobbin probe. Third, a rotating pancake coil (RPC) probe was used to confirm signals from the bobbin and 8 x 1 inspections. The RPC probe gives better resolution to small defects, but is more time consuming to employ.

The ECT inspection program was conducted utilizing state-of-the-art multifrequency eddy current test technology including the use of digital data acquisition and analysis techniques. A Westinghouse Intelligent Eddy Current Data Analysis System (IEDA) was used as an aid in flagging suspect bobbin coil indications, which were then dispositioned by data analysts. The data from each tube was independently reviewed by two different analysts. One analyst

used the Westinghouse IEDA system and the other analyst used the Zetec Digital Data Analysis System. All data analysts were certified at least Level II in accordance with American Society of Nondestructive Testing (ASNT) requirements. The analysts were given additional training by Westinghouse and required to pass a test that covers the specific data analysis used for the North Anna eddy current tests.

The ECT inspection program, including the scope of inspections, and the procedures, equipment, and techniques employed were reviewed as part of the NRC Augmented Inspection Team (AIT) which was dispatched to the North Anna site shortly after the event. The team included staff members from the NRC Office of Nuclear Reactor Regulation and an expert consultant on ECT from Oak Ridge National Laboratory. Detailed findings of the AIT investigation are documented in Reference 4. In summary, the AIT report concluded that the overall test program, the extent of the examinations, the execution of the program, and the data analysis techniques were acceptable.

In addition to the AIT effort, NRC Inspectors from Region II visited the plant on August 10, 1987 and again on August 31, 1987 to evaluate the licensee's ECT inspection and training procedures. Their findings were also favorable and are contained in Inspection Reports 50-338/87-28 (Reference 5) and 87-31 (Reference 6). On September 10, 1987, an NRR staff member and the staff's ECT consultant visited North Anna to conduct an audit of the data analysis performed on a selected set of tubes at the seventh support plate location. Based on the limited sample, the licensee's data analysis results for the upper support plate were confirmed to be adequate.

3.2 ECT Inspection Results

The North Anna plugging limit, as specified in the plant Technical Specifications, is 40% of the tube wall thickness. However, consistent with past experience, the presence of competing signals from dents and from tube expansion transitions generally precluded making accurate depth estimates for indications located at the support plates and near the top of the tubesheet. The licensee therefore plugged all tubes containing such non-quantifiable indications.

Table 1 summarizes the number of tubes plugged by indication type. All indications identified were either present in the April 1987 refueling outage with no discernible change present, or were located in previously uninspected portions of each steam generator. Additionally, a review of the data from the last outage using the current analysis rules revealed several tubes that now had a pluggable call placed on them. This apparent, though not actual, change in the steam generator condition was due to the change in the analysis rules and increased awareness by the analysts of North Anna specific ECT signals. A review and comparison of steam generator C hot leg data demonstrated that there was essentially no change in tube condition from the April 1987 refueling outage to July 1987 (when the event occurred). Finally, there were no indications of a circumferential nature found at any tube support plate locations, including the seventh tube support plates.

In addition to tubes found to contain eddy current indications, other tubes were plugged for preventive reasons as indicated in Table 1. This "preventive plugging" activity is discussed in Sections 5.2 and 5.3.

4 FAILURE ANALYSIS

A detailed failure analysis program was conducted by Westinghouse to identify the causal factors leading to the tube rupture event and to provide a basis for determining the corrective actions necessary to prevent a recurrence of this event. As part of this program, a portion of the failed tube extending from the fracture surface to the tube end on the cold leg side was removed from the steam generator for detailed laboratory examination. Section 4.1 below provides a description of these examinations which indicate that the fracture occurred as a result of fatigue. The alternating stress level leading to fatigue crack initiation was determined on the basis of observed fatigue striation spacings on the fracture surface and is discussed in Section 4.2. Section 4.3 discusses the fatigue strength properties of Inconel 600 tubes in an AVT water environment. Section 4.4 provides an assessment of the potential loading mechanisms which could have led to fatigue crack initiation and propagation. As discussed in Section 4.4, a flow-induced vibration mechanism involving a fluidelastic instability is believed to have provided the driving

Table 1 Steam generator tubes plugged as result of SGTR event (by indication type)

S/G	Clear[1] indications	Distorted[2] indications	Tube[3] sheet indications	8x1 possible[4] indications	Preventively[5] plugged	Other[6]	Total tubes plugged
A	0	6	6	11	80	2	105
B	0	3	5	12	12	1	33
C	2	2	20	11	58	19	112

[1]Clear Indications (defective) - bobbin indications of greater than 40 percent "thru-wall" depth.
[2]Distorted Indications - bobbin indications of undetermined "thru-wall" depth at the tube support plates.
[3]Tubesheet Indications - bobbin indications of undetermined "thru-wall" depth at tubesheet.
[4]8x1 Possible Indications - indications identified by 8x1 probe.
[5]Tubes plugged as a preventative measure (see Sections 5.2 and 5.3).
[6]Tubes with broken probes or which would not pass 8x1 probe - includes failed tube.

force for initiating and propagating the fatigue crack. Section 4.5 discusses various factors which are believed to have contributed to the flow instability. Based on the above, Section 4.6 provides an overall summary of the necessary conditions for causing a fatigue failure such as occurred for tube R9-C51.

4.1 Laboratory Examination of Failed Tube Specimen

4.1.1 Destructive and Non-destructive Testing

The straight section of the failed tube (R9-C51) between the fracture surface and the cold leg end was removed from steam generator C without causing significant elongation or distortion.

The results of mechanical testing and chemical analysis established that the tube had mechanical properties that met all applicable requirements (e.g., ASME Code) and otherwise displayed the expected characteristics of Alloy 600 in the mill-annealed condition. Radiography, consisting of double wall radiographs taken at four rotations 90° apart and of a single wall radiograph using a "rotisserie" technique, revealed no indications in the seventh support plate region other than the fracture at the top edge of the support plate location. Eddy current examinations were also conducted on the seventh support plate region using bobbin, 8 x 1, RPC, and outer diameter (OD) pencil probes. No indications were observed below the fracture face in the support plate region.

4.1.2 Visual and Macroscopic Examinations

With reference to Figure 1 (taken from Reference 3), which summarizes the fractographic observations schematically, the 45° location corresponds to the plane of the U-bend. Multiple fracture initiation "origins" occurred between approximately 90° and 180°. The tubing between 90° and 180° is determined to have protruded approximately 0.07 inches above the top edge of the support plate. This location is the fracture region closest in elevation to the top edge of the support plate. The highest elevation of the fracture is located at 315° and is approximately 0.17 inches above the top edge of the support plate.

On the fracture face, a dark deposit was noted from approximately 90° to 150°. Typically the deposit extends from the OD to 3/4 through-wall. An analysis of these deposits showed that they had a composition similar to adjacent OD deposits and that they contain elements which would be expected from secondary side water-borne deposits. Fatigue cracks initiated in this location. The significance of these deposits is that they may show the shape of the early macro-crack before faster crack growth rates occurred which did not leave sufficient time for disposition of water-borne material. From the shape of the deposit, it is believed that the macro-crack initially broke through-wall over a 40° crack front that extended from 100° to 140°. Fatigue striation orientation data also support this hypothesis.

Oxidation and/or fretting was observed on most of the fracture surface but was most severe at about the 135° position. It was heavy throughout the region containing most of the crack origins and of diminishing severity at locations proceeding in the clockwise direction from about 170° and counter clockwise from about 70°. This suggests that the oldest portion of the crack occurred at about the 135° position.

4.1.3 SEM and TEM Fracture Face Examination

A summary of fractographic features and striation spacing measurements is presented in Table 2 and in Figure 1, which also give the estimates of cyclic stress levels that can be made from the striation spacing as described below. Replicas or "grids" of the fracture surface were examined in a transmission electron microscope (TEM). These TEM fractographic examinations were performed to provide the resolution needed to definitively determine if the striation-like markings observed during scanning electron microscope (SEM) fractography were indeed fatigue striations and to provide quantitative data pertaining to their spacing. The striations run perpendicular to the direction of local crack propagation. The striations develop as a consequence of repeated blunting and resharpening of the crack tip during the cyclic applications of load, so each striation marks the position of the crack tip at the time it was formed. The striation spacing provides a rough estimate of the crack growth rate per cycle.

Table 2 North Anna tube fracture-summary of striation spacing measurements and ΔK calculations

Grid	Distance from O.D. surface, in.	Average spacing μ-in.	Calculated* ΔK, ksi in.
A		6.24	29.2
B		3.39	21.5
C	0.014	1.00	11.7
	0.036	1.58	14.7
	0.046	1.85	15.9
E	0.24	1.60	14.8
	0.31	1.53	14.5
F		20.7	53.2

*The ΔK-values were calculated from striation spacing measurements using: $S = 6 (\Delta K/E)^2$. (Bates and Clark[7] Correlation).

Bates and Clark (Reference 7), among others, have shown a correlation between the striation spacing and the cyclic stress intensity factor range (ΔK). Assuming that the overall vibrational loading of the tube is not significantly changed by the development and early growth of small fatigue cracks, then ΔK levels indicated from striation spacings can be used to estimate the cyclic stress range that led to fatigue crack initiation.

Scanning electron microscope (SEM) and transmission electron microscope (TEM) fractographic examinations of the fracture surface confirmed the conclusions of the optical-microscopic examinations that the crack origins were located on the outside surface. A number of "origins" were identified from fracture surface markings (tear ridges) and contours on the outside surface, with four principal initiation sites found at approximately 110°, 120°, 135° and 150°. Fine fatigue striations are observed near the crack origins. Striation spacing increased from about 1.0 micro-in. near the OD surface to nearly 2.0 micro-in. near the inner diameter (ID) surface.

The region from about 90° to 155° is generally flat (orientation: normal to wall) throughout except for small portions that have shear orientations (45° to wall) adjacent to the OD and ID surfaces, with a fine fracture texture. Most

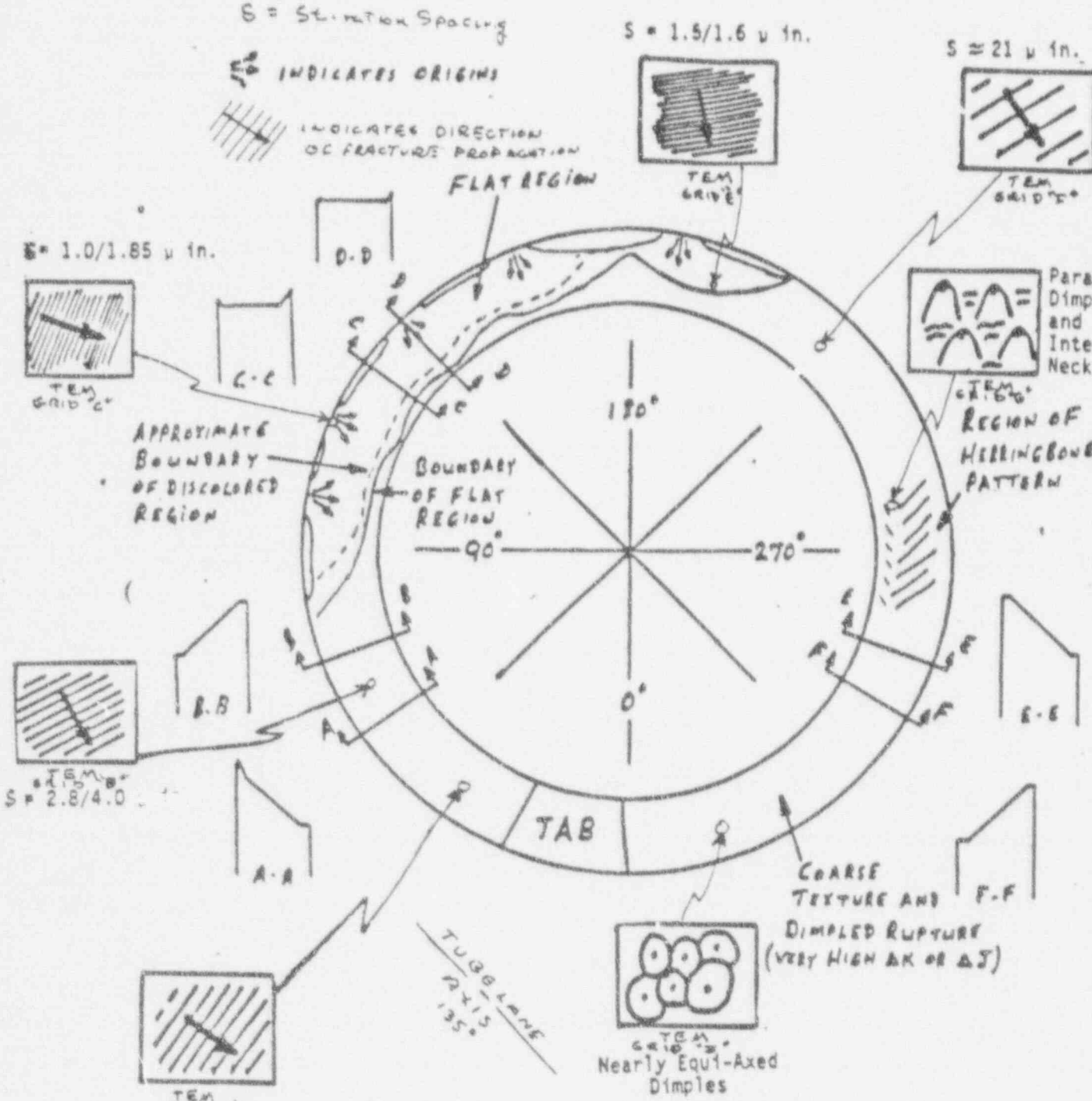

Fig. 1. Approximate Mapping of Fracture Surface of Tube R0C51, S/G 'C' Cold Leg.

of the remainder of the fracture is oriented at about 45° to the wall surface except for a flat area surrounding a minor crack origin at about the 190° location. Clockwise from 180° an initially fine texture becomes rougher with a "herringbone" pattern evident near the 270° region, indicating an accelerating rate of crack propagation.

Fine to coarse fatigue striations occur at locations from about 190° to 250° and from about 30° to 70°. The fatigue striation spacing increased (indicating higher propagation rates) as the crack propagated around the circumference of the tube in a clockwise direction from about the 190° position and counter clockwise from about the 70° position. Higher propagation rates in the 190° to 300° positions than in the 70° to 15° regions indicates eccentric loading or a component of torsional loading.

Parabolic dimples with internal necking between dimples were the predominant fractographic features at about the 270° position. These features are indicative of very high fatigue propagation rates. This position is within the regions of herringbone pattern and coarse texture observed during visual examinations.

Within the region from about 280° clockwise 360° to 15°, there is a rough texture (fractographic examination revealed dimpled rupture in this region) indicative of overload fracture. Equiaxed dimples indicative of the overload portion of the fracture were observed at about the 310° position. These fractographic features, coupled with the macroscopic features, indicate that the overload fracture occurred throughout the region defined above.

The tab-shaped area near region marked 0° has a rough fracture texture and orientation consistent with a final overload fracture.

4.1.4 Metallography of Seventh Support Plate Region

A series of longitudinal metallographic sections were made at the fracture location. Minor OD intergranular penetrations, as well as minor ID intergranular penetrations, were found in isolated, small zones within the support plate crevice region. The penetrations were typically 0.3 mils deep and approached a maximum depth of 1.0 mil. The closest distance to the fracture face, in which

an intergranular penetration approached the fracture face, was 4 mils. Although there was no direct evidence that intergranular penetrations were present at the exact fatigue initiation sites, Westinghouse notes that there remains the possibility that this could have occurred. However, Westinghouse concludes that this possibility does not change the observed data which supports fatigue as the mechanism for crack initiation and propagation.

4.2 Fatigue Crack Initiation Stress

Westinghouse estimates that an alternating stress amplitude of 4 to 10 ksi was necessary for crack initiation. Among the evidence cited by Westinghouse in support of this estimate was the following:

(1) Use of a single edge crack model indicates an alternating stress of 6.3 ksi for a crack penetrating 50% through-wall and assuming a ΔK of 13 ksi $\sqrt{in.}$ (see Table 2) and an R ratio (i.e., Kmin/Kmax) of 0.5 (Reference 3).

(2) A cyclic fatigue test of a tube specimen was conducted at a known stress amplitude. Based on a comparison of the striation spacings between the test specimen and the fracture surface of tube R9-C51, an alternating stress of 8 ksi was estimated for R9-C51 (Reference 8).

(3) Based on the observed striation spacings and use of the stress intensity expression taken from Section 33.2 of the Tada, Paris, Irwin handbook, the alternating stress level is estimated to have been about 5 to 7 ksi at the time the crack penetrated entirely through-wall and had begun to propagate around the tube circumference (Reference 3).

With respect to item 1 above, a Westinghouse representative indicated during a phone conversation with an NRC staff consultant that 4 ksi was judged to be a reasonable lower bound alternating stress to account for potential uncertainties in the use of the single edge crack model and the assumed R ratio. With respect to item 3 above, the Westinghouse representative stated that 10 ksi was the

maximum possible value of alternating stress consistent with the Δk = 53 ksi $\sqrt{in.}$ estimate shown in Table 2 (assumed to be located 90° relative to the point of crack initiation) without resulting in a physically impossible stress history during crack propagation (Reference 9).

4.3 Fatigue Strength

"S/N curves" are curves relating the magnitude of alternating stress to the number of alternating stress cycles necessary to initiate a fatigue crack. The S/N curves used by Westinghouse to evaluate conditions for crack initiation were taken from data in [ ]. This data is based on fully reversed loading. As will be discussed in additional detail later in this report, a flow-induced, tube vibration mechanism is believed to be the driving mechanism for both fatigue crack initiation and crack propagation. The natural frequency of the row 9 tube U-bends is about [ ]. Assuming that the fatigue crack initiated over a period ranging between one year and the 9-year lifetime of the plant to date, then the number of loading cycles leading to fatigue failure (assuming a plant availability factor of 75%) was between 1.4×10^9 cycles and 1.3×10^{10} cycles. The corresponding fatigue strengths are estimated by the staff to be 27 ksi and 22 ksi utilizing a best fit S/N curve from the data in Reference 10 and 21 ksi and 16 ksi, respectively, when a 3 standard deviation (3σ) lower bound S/N curve is used. These fatigue strength estimates exceed the 4 to 10 ksi alternating stress believed by Westinghouse to have caused fatigue crack initiation (see Section 4.2), but do not include an adjustment for mean stress at the fracture location induced by denting of the tube at the seventh support plate.

The mean stress at the fracture location was evaluated by Westinghouse with an elastic-plastic finite element analysis utilizing an axi-symmetric model. The assumed denting deflection profile from the bottom of the seventh support plate to the top was based on profilometry measurements conducted on the fractured tube and other adjacent tubes. The fractured tube had a maximum radial displacement of 2.5 mils. Steady state pressure and thermal loadings were also

included in the model. The results of the analysis revealed a tensile mean stress level at the tube OD at the yield strength level.

The [ ] was used to make the mean stress adjustment to the S/N curves derived from the EPRI data. [

]

Table 3 provides a summary of alternating stress levels associated with assumed fatigue crack initiation over a 1-year and 9-year period, respectively, for a best fit, 2σ, and 3σ S/N curve incorporating the mean stress adjustment.

Table 3 Alternating Stress Levels Leading to Fatigue Crack Initiation

	1.4×10^9 cycles (1 year)	1.3×10^{10} cycles (9 years)
Best fit S/N Curve	13.3 Ksi*	9.2 Ksi*
2σ S/N Curve	10.5 Ksi	7 Ksi
3σ S/N Curve	8.7 Ksi	5.6 Ksi

*These estimates were made by the NRC staff.

The tabulated stresses associated with fatigue crack initiation over a 9-year period are consistent with the Westinghouse estimated range of 4 to 10 ksi required for crack initiation. The tabulated stresses associated with crack initiation over a one-year period exceed this range if best fit or 2σ S/N properties are assumed. Thus, if best fit or 2σ S/N properties are assumed, then the cyclic loadings leading to crack initiation must have occurred during a period exceeding 1 year.

4.4 Potential Loading Mechanisms Leading to Fatigue Crack Initiation and Failure

It is evident from the observed striations on the R9-C51 fracture surface that at least 10^5 load cycles were required to propagate the crack to failure subsequent to crack initiation. Based on primary-to-secondary leak rates prior to the rupture event, it appears that the crack propagated rapidly to failure over just a few days. Potential loading mechanisms for crack initiation and/or propagation considered by Westinghouse are described below.

4.4.1 Duty Cycles Associated With Normal, Upset, and Test Conditions

Applicable duty cycles for normal, upset, and plant test conditions considered by Westinghouse were taken from the North Anna steam generator design specifications. Examples of the types of duty cycles considered include plant heatups and cooldowns, various plant loading transients, feedwater transients, reactor trips, steam line breaks, and plant hydrostatic tests. The various duty cycles included contributions from differential pressure loadings across the tube walls, interference loads from differential radial expansion between the tube and support plate, and through-wall thermal gradients in the tube.

These duty cycles were analyzed using an axisymmetric finite element model of the tube. Alternating stress levels ranged from [

] The total number of stress cycles, however, is estimated to be less than 40,000 cycles for the entire 40 year lifetime of the plant. Thus, the plant duty cycles were found to contribute very little to fatigue usage (i.e., usage factor = 0.04 over 40 year plant lifetime), and are not believed to have played a significant role in initiating or propagating the crack.

4.4.2 Flow Induced Vibration

Potential flow induced vibration mechanisms considered by Westinghouse including vortex shedding, cross flow turbulence, and fluid-elastic instability.

[

]

The Westinghouse analysis of linear turbulence and fluidelastic excitation of the tubing was conducted with a computer program called FLOVIB. FLOVIB incorporates a finite element model of the tube and tube support system and evaluates the dynamic response of the tube based on models for modal vibration amplitude in the turbulent and fluidelastic regimes.

[

]

The above mentioned model for evaluating tube response from the turbulence mechanism has reportedly been qualified against several series of tests including prototypical two-phase tests. Turbulence induced vibration amplitudes for tube R9-C51 are predicted to be on the order of less than [

] at the tube apex. This order of amplitude would cause maximum stresses in the top of the uppermost support plate (where the rupture occurred) with peak-to-peak amplitudes of less than 1000 psi. Based on these low stress levels, Westinghouse believes it to be highly improbable that the turbulence mechanism is primarily responsible for the North Anna tube rupture.

The fluidelastic mechanism will have a significant effect on the tube response in cases where the fluidelastic stability ratio (SR) equals or exceeds 1.0. The stability ratio is defined as

$$SR = \frac{V_{eff}}{V_c}$$

where V_{eff} is the effective crossflow velocity and V_c is the critical velocity beyond which the displacement response increases rapidly.

The estimated stability ratio [ ] utilizing nominal estimates of parameters such as damping ratio, stability constant, and natural frequency is [ ] indicating no fluidelastic instability. As will discussed later, these parameters are subject to significant uncertainties (particularly for damping ratio) such that depending on the actual values of the parameters, the stability ratio may substantially exceed 1.0.

Motions and corresponding stresses developed by a tube in the fluidelastically unstable mode are quite large in comparison to the other known mechanisms. For this reason, and because none of the other mechanisms discussed above appear to be a plausible mechanism for crack initiation, Westinghouse has concluded that the failed tube is most likely a result of its being fluidelastically unstable.

Given fluidelastic instability as the mechanism for fatigue crack initiation, the stability ratios for the failed tube can be inferred from [

]

To estimate the critical velocity and, hence, the stability ratios of the tube which failed, its is helpful to consider Figure 2. [

]

From experimental results, Westinghouse states that [

]

As can be seen from Figure 2, definition of points 1 and 2 and the slopes of the turbulence and fluidelastic response curves are sufficient to solve for Vc and thus for stability ratio (i.e., V_{oper}/Vc). On this basis, tube R9-C51 is estimated to have been operating (prior to crack initiation) at a stability ratio in the range of 1.22 (slope of 20) to 1.56 (slope of 10), assuming the tube to be vibrating with a displacement amplitude of 0.057 inches and a corresponding alternating stress level of 7 ksi.

It follows from Figure 2 that for a given reduction in stability ratio from SR_2 to SR_1, the corresponding reduction in displacement (i.e., from D_2 to D_1) response and alternating stress can be expressed as follows:

[ ]

It can be seen from this equation that a small percentage reduction in stability ratio will lead to a much larger percentage reduction in displacement response and alternating stress. With a known reduction in alternating stress, the corresponding reduced value of fatigue usage factor can be estimated from the appropriate S/N curve.

It is useful for purposes of later discussion to tabulate reductions in alternating stress level and fatigue usage accumulation as a function of percentage

Figure 2

reduction in stability ratio. Tables 4 and 5 summarize these reductions for different S/N curve assumptions based on an assumed time to initiate a fatigue crack in R9-C51 of one year and 9 years, respectively. These reductions have been conservatively estimated assuming a slope of 10 for the fluidelastic response curve when the displacement response exceeds 40 mils, and a slope of 6 when the displacement response is less than 40 mils.

4.5 Causes of High Stability Ratios

As discussed in Section 4.4.2, the estimated stability ratio for tube R9-C51 is [ ] using nominal estimates of parameters such as stability constant, natural frequency, and damping ratio. Thus the tube would have been expected to be stable with considerable margin. The following summarizes Westinghouse's assessment (Reference 3) of factors which may have caused the actual stability ratio to significantly exceed 1.

Average Flow Field, Stability Constant, and Natural Frequency Uncertainties

Westinghouse estimates that uncertainties in the average flow field, stability constant, and natural frequencies are essentially the same for units with dented or non-dented support plates. If these errors were large, Westinghouse believes that similar instabilities would be expected in the non-dented units with resulting wear at either the top support plate or inner row AVBs. Since such wear has not been observed in rows 8 to 10 in non-dented units, Westinghouse believes the potential uncertainties to be relatively small (about 15%) and, therefore, not a major contributor to the failure of R9-C51.

Local Flow Velocities

The eddy current test results revealed that the AVB supports generally extended as far as row 10 with most extending at least as far as row 9 and many as far as row 8. These non-uniform AVB penetrations are believed by Westinghouse to have channeled some of the flow to row 8 and row 9 tubes without adjacent AVB supports causing a "velocity peaking" effect for

Table 4 Alternating stress and fatigue usage sensitivity to stability ratio reductions (assuming 1.4×10^9 cycles to failure for R9-C51)

	S/N Curve Assumptions		
	Best Fit	2σ	3σ
Pre-mod alt. stress	13.3 ksi*	10.5 ksi	8.7 ksi
Post-mod alt. stress (10% reduction in SR)	NE	4.2 ksi	3.8 ksi
Additional accumulated usage factor over remaining 31 years of plant life	NE	0.20	0.52
Post-mod alt. stress (15% reduction in SR)	NE	3.0 ksi*	2.6 ksi*
Additional accumulated usage factor over remaining 31 years of plant life	NE	Negligible*	0.10*

*NRC staff estimates
NE ~ Not estimated

Table 5 Alternating stress and fatigue usage sensitivity to stability ratio reductions (assuming 1.3×10^{10} cycles to failure for R9-C51)

	S/N Curve Assumptions		
	Best Fit	2σ	3σ
Pre-mod alt. stress	9.2 ksi*	7 ksi	5.6 ksi
Post-mod alt. stress (10% reduction in SR)	3.8 ksi*	3.2 ksi	2.8 ksi
Additional accumulated usage factor over remaining 31 years of plant life	Negligible*	0.06	0.10
Post-mod alt. stress (15% reduction in SR)	2.7 ksi*	2.3 ksi*	2.0 ksi*
Additional accumulated usage factor over remaining 31 years of plant life	Negligible*	Negligible*	Negligible*

*NRC staff estimates.

these tubes. Westinghouse has provided a preliminary estimate of a 15% velocity peaking factor for tube R9-C51 (Reference 3). However, a few row 8 to row 10 tubes were found to contain wall thinning indications (possibly wear from AVBs) which may have occurred as a result of fluid-elastic excitation. Some of these tubes were located in regions of relatively uniform AVB penetrations. Thus, Westinghouse concludes in Reference 3 that non-uniform AVBs and local flow effects are not the dominant factor for instability although this effect at a 15% magnitude could have had a major contributing influence on the R9-C51 failure.

Tube Damping Uncertainties

Westinghouse concluded in Reference 3 that tube damping ratio uncertainties were the dominant factor affecting the stability ratio of the row 9 U-bends. Measurements of mechanical damping in air were performed using a U-bend shaker test facility. For [

] The measured mechanical damping was observed to increase substantially as the support conditions were gradually relaxed, reaching a value of 1.1% for preloaded, pinned-pinned supports typical of U-bend steam generator conditions without denting.

The above air tests do not consider the additional damping in a two-phase water/steam environment. Data cited by Westinghouse shows [

] However, Westinghouse concluded in Reference 3 that the effects of denting on tube

damping appear to be the major uncertainty factor leading to tube instabilities. Westinghouse estimates a 50% uncertainty factor associated with the assumed 0.82% damping ratio which would contribute approximately 41% uncertainty to the nominal stability ratio estimate. Westinghouse further notes that an assumed lower bound damping ratio estimate of [ ] would double the nominal stability ratio estimate.

4.6 Required Conditions for Fatigue Cracking Initiation

Westinghouse has reached the following conclusions regarding the conditions necessary for fatigue crack initiation.

(1) Denting at the top support plate is needed to (a) produce a high mean stress effect with an associated reduction in fatigue strength, (b) maximize bending stress at the upper support plate, and (c) minimize tube damping.

(2) An absence of adjacent AVB supports is needed in order that tube displacements and, thus, alternating stress levels may be large enough to initiate a fatigue crack.

(3) Stability ratios within 10% of that for tube R9-C51 (i.e., stability ratios $\geq$ 90% of that for tube R9-C51) are needed since lower values are too small to initiate fatigue cracking.

(4) Off-nominal conditions for fluid elastic vibrations are necessary including either or both of the following: (a) tube damping below test measurements [ ] approaching mechanical damping only [ ] and (b) locally high flow velocity regions.

5 CORRECTIVE ACTIONS AND COMPENSATORY MEASURES

The licensee has taken a two-fold approach to preclude future fatigue crack initiation; namely (1) installation of a steam generator downcomer flow

resistance plate as discussed in Section 5.1 and (2) implementation of preventive plugging of tubes with potentially high stability ratios as discussed in Section 5.2. Section 5.3 discusses actions taken to stabilize the remnant portion of tube R9-C51 (i.e., the ruptured tube) to ensure that it does not cause subsequent damage to adjacent tubes. Section 5.4 discusses the licensee's enhanced primary-to-secondary leak rate monitoring program which is intended to provide added assurance of steam generator tube integrity.

5.1 Downcomer Flow Resistance Plate (DFRP)

The DFRP is an annular, perforated plate located near the top of the downcomer annulus between the wrapper and shell of the steam generator. Installation of the DFRP will reduce the steam generator circulation ratio from 4.3 to 2.9 with an accompanying reduction in crossflow velocities and stability ratios for all tubes. As discussed in Section 4.6, low damping conditions are concluded by Westinghouse to be the primary contributor to fluid elastic instabilities. For tubes with low damping ratios, installation of the DFRP is calculated to produce between a 13% and 22% reduction in stability ratio, exceeding the 10% reduction objective set by Westinghouse. For tubes with nominal damping, an 8% reduction in stability ratio is estimated.

5.2 Preventive Plugging

Although installation of the DFRP is believed by Westinghouse to be a sufficient measure to preclude fatigue crack initiation in the future, preventive plugging of "susceptible" tubes in rows 9, 10, and 11 has been performed. A susceptible tube is one which is not supported by AVBs and is in a region of locally high flow velocities. All tubes above row 11 have AVB support. As discussed previously, many tubes down to row 8 are known from eddy current testing to be supported by AVBs. Tubes in row 8 and below, even if not supported by AVBs, have stability ratios at least 14% less than that of tube R9-C51 by virtue of their shorter span lengths (between supports) and associated higher natural frequency. Thus, tubes in rows 8 and below meet Westinghouse's 10% criterion (see Section 4.6), even without consideration of the additional reduction in stability ratio associated with the DFRP modification.

Based on the above, potentially susceptible tubes were considered by Westinghouse to be located in rows 9, 10, and 11. The detection of an AVB signal is considered by Westinghouse to be a firm indication of an AVB support on at least one side. Test data was presented demonstrating that the vibration amplitude for a given tube is controlled by the AVB exhibiting the minimum radial gap with respect to that tube. Thus, Westinghouse maintains that an AVB support on one side only will constitute a fully effective AVB support.

It is possible for eddy current testing to miss the presence of an effective AVB support due to background noise conditions such as from upper surface deposits. In some cases, however, the actual presence of an AVB support can be inferred from an AVB support detected for an adjacent tube. For example, it can reasonably be inferred from an AVB indication for a row 8 tube that the adjacent row 9 tube (in the same column) also has an AVB support regardless of whether that tube exhibited a detectable AVB indication.

The plugging of all susceptible tubes in rows 9, 10, and 11 would have the effect of leaving tubes in row 8 as the tubes with the most limiting stability ratio. Therefore, this action by itself is estimated by Westinghouse to result in a 14% reduction in stability ratio relative to R9-C51. In addition, Westinghouse has estimated on the basis of a preliminary analysis of the local high flow velocity regions as affected by nonuniform AVB insertion that velocity peaking factors are lower for row 8 tubes than for the most limiting susceptible row 9 tubes. This effect is estimated by Westinghouse to produce an additional 6% reduction in stability ratio associated with the plugging of susceptible tubes in rows 9, 10, and 11.

The staff's review of the licensee's preventive plugging program identified two tubes in row 9 of S/G A considered by the staff to be in the category of "susceptible tubes" (i.e., tubes R9-C38 and R9-C54), but which had not been preventively plugged. Neither of these tubes could be confirmed on the basis of the eddy current data to be supported by AVBs. In addition, the absence of AVB supports for these tubes could, in the staff's opinion, subject these tubes to locally high flow velocities due to channeling effects caused by nonuniform

AVB penetrations. At the staff's request, the licensee agreed to include these tubes in its preventive plugging program (Reference 6).

The staff also identified a concern to the licensee (during telephone conversations) that no criteria existed to ensure that an AVB signal represented an effective AVB support. The nominal radial clearance between the AVBs and adjacent tubes is about 10 mils. However, unless the AVB extends all the way down to at least the centerline of the tube, the tube will have additional freedom to displace laterally depending on exactly how far the AVB actually penetrates. Thus, a concern existed that AVBs may be sufficiently close to the tube to produce a detectable eddy current signal, but not be effective in limiting tube displacements to less than the estimated 0.032 to 0.080 inch range associated with fatigue crack initiation and failure of tube R9-C51.

In response to the staff's concern, the licensee reviewed the eddy current tapes for all row 9 tubes for which the adjacent row 8 tubes exhibited no detectable AVB indication. (In cases where row 8 tubes exhibited an AVB signal, it can be reasonably inferred that at least one AVB penetrates below the centerline of the adjacent row 9 tube, thus ensuring a fully effective AVB support.) The presence of two discrete AVB signals (on the hot and cold leg side of the apex) was interpreted by the licensee to be indicative of at least one AVB intersecting the tube U-bend below the tube centerline at the apex, thus ensuring a fully effective (i.e., fully penetrated) AVB support. However, the review of the eddy current tapes for the subject tube revealed 41 tubes not exhibiting the two discrete AVB signals. In the absence of criteria for evaluating the acceptability of AVB indications for these tubes, the licensee conservatively elected to expand the preventive plugging program to include these 41 tubes.

Preventive plugging of susceptible tubes has been accomplished using a "sentinel plug" on the cold leg side and a standard mechanical plug on the hot leg side. The sentinel plug contains a hole to permit internal pressurization of the tube and low level primary to secondary leakage in the event that a through-wall crack develops in the tube. The hole is sized to permit detectable leakage in excess of the administratively imposed limit of 100 gallons per day

(gpd), but well under the 500 gpd Technical Specification limits. This plug is intended to serve as an early warning detection method of a circumferential break of the plugged tube prior to its potential interaction with adjacent tubes.

5.3 Stabilization of Severed Tube, R9-C51

After removing the cold leg section of tubing from the steam generator (see Section 4), only the hot leg remnant of the tube including the U-bend portion remained in the steam generator. Thermal-hydraulic analysis of the flow conditions surrounding tube R9-C51 indicated that the severed tube U-bend would be fluid elastically unstable during power operation. Once unstable, the remnant section could then impact neighboring tubes and over time cause wear on the neighboring tubes. Therefore, a stabilization technique was developed to secure the tube remnant from the cold leg side. Specifically, a threaded assembly (jointed spear) was designed and manufactured for insertion into the cold leg tubesheet and support plate hole. The assembly featured the following: (1) eight threaded sections, each assembled and inserted into the bare hole, (2) a locking feature to preclude separation of the threaded sections, (3) hydraulic expansions at each tube support plate and into the free end of remnant tube R9-C51, and (4) a roll expansion attachment of the spear to the tubesheet.

The design of the jointed spear components was verified by a combination of physical tests and computer analysis. These tests included torque and bending tests on the spear to remnant tube joint and axial separation (pull) tests and cyclic loading tests on both the threaded joint and on the spear to remnant joint. Analyses were performed to quantify the tube/spear vibrational characteristics. These analyses demonstrated that the critical components (threaded joints and spear to remnant joint) would withstand the design bases operational and transient induced forces. Additionally, due to the small gap between the seventh support plate and the spear, damping would be higher and therefore reduce the loadings and susceptibility of the spear to a fatigue failure.

A full-scale mockup of tube R9-C51 was made at Westinghouse to ensure that the installation of the jointed spear on the cold leg side could be performed successfully.

Installation of the jointed spear was to be accomplished as follows:

[

]

As a preventive measure, it was determined to stabilize the hot leg portion of the remnant tube. Stabilization of the hot leg was to be performed by using a flexible [ ] cable with [

] The stabilizer is then inserted into the remnant tube and extends over three inches above the top of the hot leg seventh support plate and slightly into the U-bend. [

]

No specific verification analyses were performed for the hot leg stabilizer to be used at North Anna Unit 1 since this type of design has been previously tested, qualified, and used by Westinghouse at other facilities.

After completing the installation process described above, the spear was then eddy-current tested to confirm the existence and proper positioning of the expansions.

The method of stabilization was modified from the above description to account for difficulties encountered during installation.

When the spear described above was expanded into the seventh tube support plate on the cold leg side, the expanding tool was slightly out of position and ruptured the spear wall over a length of about 1/2 inch. The crack was axial in nature and occurred near the top of the seventh tube support plate. Fracture and thermal-hydraulic analyses were conducted and it was then determined to install a sleeve inside the spear spanning the distance from the tube remnant to the seventh tube support plate. This sleeve was approximately 13 inches in length and extended from about 3 inches inside the tube remnant to about 9 inches below the seventh tube support plate. The bare hole in the tube sheet (cold leg) was sealed with a welded plug.

During installation of the cable stabilizer on the hot leg side, one of the cable sections was damaged when the stabilizer jammed on the base plate of the insertion tool. The damaged stabilizer was removed, the base plate was modified, and a second stabilizer, identical to the first, was then successfully installed. The cable stabilizer extends from the hot leg tube sheet to approximately 30° past the tangent point at the hot leg U-bend. The hot leg tube end was then sealed with a mechanical plug.

Finally, twelve adjacent tubes around tube R9C51 were preventively plugged with sentinel plugs on the cold leg side. On the hot leg side, tube R9-C51 was plugged with a solid mechanical plug.

5.4 Leak-Before-Break Considerations

Prior to the failure of tube R9-C51 on July 15, 1987, the control room operators had no indication on the instrumentation normally used to detect primary to secondary leakage. However, a post-event analysis of air ejector radiation monitor count rate data and air ejector grab sample data did reveal indications of leakage prior to the event (Reference 3). These data were subject to some error because of the manner in which they were obtained, and the licensee has noted (in the context of discussion of the air ejector radiation monitor data) that the data should not be used to quantify a specific leak rate at a given point in time. However, these data give a positive indication that leakage was present for at least 48 hours prior to the event and that it was trending upward.

The licensee has taken a number of actions to ensure that similar precursor leakage in the future will be detected and monitored such that the plant will be shut down before a gross rupture of the tube can occur. These actions include:

(1) primary-to-secondary leakage will be estimated every 4 hours using the air ejector radiation monitor, S/G blowdown monitor, and N-16 monitor; every 8 hours using the air ejector exhaust isotopic activity; and every 24 hours based on secondary coolant isotopic activity. The alarm setpoint for the air ejector monitor will be adjusted to respond if leakage increases and stays 10 to 20 gpd above the most recent leakage measurement.

(2) N-16 monitors are being installed to provide a diverse indicator of primary-to-secondary leakage. The N-16 monitor will have a continuous readout (in gallons per day) in the control room and three pre-set alarms. The first alarm (S1) will be set consistent with the air ejector radiation monitor alarm above. The second alarm (S2) will be set at 60 gpd in order to detect the initial crack propagation associated with a fatigue failure. The third alarm (SE) will be set at the administratively imposed shutdown limit of 100 gpd.

As part of North Anna Power Station Standing Order #155 (Revision 1), dated October 9, 1987, the licensee has set the following administrative limits on primary to secondary leakage.

a) 100 gpd per S/G, 300 gpd total for all S/Gs. (This is substantially more conservative than the 500 gpd limit per S/G and the 1 gallon per minute (gpm) (about 1430 gpd) limit for total primary to secondary leakage (i.e., for all S/Gs) in the Technical Specifications).

b) 60 gpd increase during any 4-hour surveillance period (applies to leakage from each S/G and total leakage from all S/Gs).

c) An increasing trend based on the latest surveillance indicating that leakage will exceed 100 gpd within 90 minutes.

If any of the above limits are exceeded, then power will be reduced to less than 50% within 90 minutes. Analysis by the licensee indicates that this should be sufficient to cause further crack propagation to cease. In addition, the plant must be brought to a hot shutdown condition within 6 hours if the limits in items b) or c) above have been exceeded.

Analyses have been conducted by Westinghouse and the licensee to demonstrate that the 100 gpd administrative limit provides adequate assurance that crack propagation will be terminated and that the plant will be shut down before rupture occurs. Leakage rate versus time curves have been calculated on the basis of predicted crack growth rates and Westinghouse test data concerning leak rates as a function of crack arc-length. These curves vary as a function of alternating stress.

From the leak rate versus time curves, the licensee estimates that a 333 gpd limit would provide the approximately 90 minute period needed to identify excessive leakage and to reduce power to 50%, assuming an alternating stress level of 7 ksi, prior to rupture of the tube. Post modification alternating stress levels, even assuming only a 10% reduction in stability ratio, are predicted to less than 7 ksi. The 333 gpd limit would also allow for a ±50% error band

associated with the N-16 monitor reading, whereas the licensee estimates the actual error band to be between ±10% and ±30%. Thus, the licensee concludes the 100 gpd administrative limit to be conservative.

Detailed procedures have been written for logging and trending data in accordance with the time schedules indicated above and for responding to the various alarms (S1, S2, and SE). Activation of the S1, S2, or SE alarms will cause the operator to be referred to the administrative limits in Standing Order 155. The staff notes that (in the event of an S1 or S2 alarm) this would include a new trending analysis to ensure that the 100 gpd administrative limits would not be exceeded over the next 90-minute period.

NRR staff representatives reviewed these procedures and witnessed (from the control room) implementation of the leak rate surveillance procedures for a typical 4-hour surveillance interval. This included the logging of the leak rate data provided directly and continuously by the N-16 monitor, the logging of count rate data from the air ejector and S/G radiation monitors and calculation of corresponding leakage rates, and checking the setpoints of the various alarms. Trending plots were generated by computer. Based on its review, the staff concludes the leak rate surveillance schedules and procedures will be effective for purposes of early detection of low level primary to secondary leakage which could be a precursor to an impending fatigue failure. The administrative leak rate limits provide added assurance that the plant will be shut down in a timely fashion before a leaking throughwall crack can propagate to failure.

6 STAFF FINDINGS

1. The eddy current test program encompassed all unplugged tubes in the steam generators in both the hot and cold leg sides. The test equipment and probes and data analysis techniques were fully state of the art and appropriate for the intended application; namely the detection of cracks at the tube support plates and tubesheet and in particular, circumferential fatigue cracks at the seventh support plate. The additional training given to data evaluators (focusing on the North Anna circumstances) and the

independent data analyses by different data evaluators using different data analysis equipment provide added assurance that the inspection program identified all tubes with potentially significant indications.

2. The presence of clearly identifiable fatigue striations as well as other features associated with fatigue leaves no doubt that the failure of R9-C51 was caused by fatigue.

3. The possibility that intergranular attack (IGA) may have contributed to fatigue crack initiation cannot be entirely discounted in view of small (1 or 2 grains) IGA penetrations observed as close as 4 mils from the fracture surface. Qualitatively, any such influence would be in the direction of reducing the alternating stress needed to initiate a fatigue crack over a given period time, but there is no data available to quantify this effect. Even if an IGA influence is assumed, however, it in no way detracts from the effectiveness of the corrective actions being taken to reduce alternating stress levels and the corresponding potential for fatigue, and thus does not affect the conclusions of this Safety Evaluation.

4. An independent calculation by one of the NRC staff consultants was consistent with Westinghouse's conclusion regarding the presence of a mean stress of approximately yield stress at the location of crack initiation. This calculation utilized a model for stress intensity factor (K) in a thin-walled tube containing a thumbnail crack initiating from the O.D. (Reference 9). The solution for K does not include the effects of bending, but is judged to be applicable to the conditions under consideration for very shallow crack depths where the axial stress gradient is small. Based on an assumed crack depth of 0.0025 inch and a K max equal to 4 Ksi $\sqrt{in.}$, this model predicts a "far field" stress of [ ] Ksi which is very close to the yield strength of the tube R9-C51 material. The K max assumption is consistent with the fractographic evidence observed by the consultant on the failed tube near the crack origin.

5. The 4 to 10 Ksi alternating stress estimate by Westinghouse for tube R9-C51 appears reasonable. The fatigue crack is estimated by the staff to have initiated over a period of between 3 and 9 years based on the

length of time the requisite denting at the seventh support plate was present. (This is based on the fact that denting was first observed at North Anna Unit 1 in 1979 and reportedly has been arrested since at least 1984.) Upon initiation, the crack propagated very rapidly (over a period of just a few days) to failure. Thus, the fact that eddy current testing revealed no other tubes with circumferential cracks at the seventh support plate is not surprising.

6. Fluidelastic instability has reasonably been established as the only credible mechanism for producing displacements of sufficient magnitude to cause a fatigue failure. Further, it has reasonably been demonstrated that such an instability is possible within the uncertainties of key parameters such as damping, velocity peaking factors, stability constant, and natural frequency cited by Westinghouse.

7. Given the complexity of the problem (e.g., two phase flow, U-tubes, denting) and the associated uncertainties, the Westinghouse analyses conducted with ATHOS AND FLOVIB provide only "ballpark estimates" of the response amplitudes and instability thresholds. Absolute values of predicted critical velocities and displacement amplitudes in the instability region incorporate significant uncertainty. However, the results of these analyses are appropriate for the use that Westinghouse has made of them; namely to examine trends, to develop relationships between changes in stability ratio and resulting changes in displacement and alternating stress response, and to evaluate relative improvements associated with installation of the downcomer flow resistance plate.

8. The predicted 8 to 22% reduction in stability ratio associated with the DFRP is judged to be reasonable since, again, it is the relative change in stability ratio that is of interest. Pertinent parameters such as density and effective flow velocities are calculated by the same method for both the pre-modification and post-modification conditions, thus minimizing the impact of any uncertainties regarding the values of these parameters. Predictions regarding the percent reduction in displacement and alternating stress are considered to be reasonable since they are based on conservative values of the fluidelastic response curve slopes.

9. Because the pre-modification stability ratio of tube R9-C51 is very uncertain, the 8 to 22% reduction in stability ratio associated with the DFRP and the additional 14% to 20% reduction associated with the preventive plugging of "susceptible tubes" in rows 9, 10, and 11 may or may not be sufficient to reduce the maximum stability ratio to less than 1.0. Even if the stability ratio exceeds 1.0, however, the expected reductions in displacement, alternating stress, and rate of fatigue usage accumulation are considered by the staff to be sufficient to preclude another fatigue failure in the future.

10. Apart from tube R9-C51 which failed, it is entirely possible that other tubes in row 9, 10, or 11 which may not have been effectively supported by AVBs and which may have been subject to locally high flow velocities may have developed significant fatigue usage factors at the time of the R9-C51 failure. Although installation of the DFRP is expected to significantly reduce the rate of future fatigue usage accumulation, it does nothing to mitigate fatigue usage which may have already have accumulated to date. Thus, actions taken to preventively plug susceptible tubes may be even more important than the DFRP is preventing future fatigue failures. Assuming that all susceptible tubes in rows 9, 10, and 11 have been plugged and considering that stability ratios for row 8 tubes are at least 14% to 20% less than that for R9-C51, the staff estimates that the fatigue usage factor for the most limiting row 8 tubes have not exceeded 0.03 to date which is well within acceptable limits. Furthermore, assuming a stability ratio reduction of 8% as a result of the DFRP installation, the staff estimates that fatigue usage for row 8 tubes will exhibit negligible incremental increase during the remaining 31 years of plant life.

11. During a meeting with the staff on November 4, 1987 (Reference 12) Westinghouse reported that recent test results indicate that the flow peaking factor for tube K9-C51 may have exceeded 30%, compared to the 15% assumed in Reference 3. This information suggests that flow peaking factors may have played a more important role, and damping ratio uncertainties a less important role in contributing to the tube rupture than was indicated in Reference 3. This new information is currently being reviewed by the staff. However, assuming this information to be valid, stability ratio reductions

associated with preventive plugging would be expected by the staff to be higher than the 14 to 20% estimated by Westinghouse in Reference 3 since preventive plugging would be expected to significantly reduce flow peaking. The staff concludes that the overall stability ratio reductions estimated by Westinghouse in Reference 3, based on the corrective actions implemented by the licensee, are conservative.

12. Actions taken by the licensee to augment its preventive plugging program to address staff concerns, as discussed in Section 5.2, are considered acceptable by the staff and provide added assurance that tubes without fully effective AVB supports in rows 9, 10, and 11 have been removed from service.

13. The use of sentinel plug for "susceptible tubes" precludes a recurrence of the Ginna syndrome (NUREG-916); namely, fracture of a tube subsequent to its being plugged leading to damage and perhaps rupture of adjacent unplugged tubes without prior indication of primary to secondary leakage. Because the population of tubes with the sentinel plugs includes the tubes in the bundle most susceptible to large amplitude vibration, any future fatigue cracks would likely affect tubes in this population producing detectable but small, controlled leakage before affecting non-plugged tubes. Thus, the tubes with sentinel plugs installed will also serve as a long term indication of the effectiveness of DFRP minimizing large amplitude vibrations and alternating stress levels.

14. Stabilization of tube R9-C51 on the cold leg side has been determined to be acceptable based on physical tests and computer analyses. The analyses have determined that the jointed spear which was inserted in the R9-C51 cold leg remnant above the seventh support plate level meets design bases operational and transient induced forces. In addition, damping will be higher and thus reduce the loadings and susceptibility of the spear stabilization mechanism to any fatigue failure. For the hot leg side, the design and use of the flexible steel cable design has previously been tested, qualified, and used at other facilities. Finally, for the cold leg side, tubes adjacent to tube R9-C51 have been plugged with sentinel tubes to

mitigate the impact of unlikely wear on neighboring tubes. Based on the above, the staff finds that the stabilization analyses and techniques used are acceptable to stabilize the R9-C51 tube remnant on both the cold and hot leg side.

15. The staff has evaluated licensee capabilities and procedures for monitoring primary to secondary leakage, and participated in an onsite walk-through of a 4-hour surveillance cycle and trending analysis. The staff finds that the licensee has substantially improved its capabilities to detect and monitor low level primary to secondary leakage which could potentially be a precursor to a similar tube rupture in the future. The licensee has adopted an administrative limit of 100 gpd which is significantly more restrictive than the standard Technical Specification limit of 500 gpd and which provides added assurance that the plant will be shut down in a timely fashion before a leaking through wall crack can propagate to failure.

7 CONCLUSIONS

Based on the above evaluation, the staff finds that the licensee has (1) adequately demonstrated the primary failure mechanism leading to the July 15, 1987 SGTR event to be fatigue caused by flow induced vibration, (2) adequately identified the major causal factors leading to this event, and (3) implemented acceptable diagnostic and corrective measures to prevent a similar fatigue failure in future. The staff concludes that the steam generators have been restored to an acceptable condition from a steam generator tube integrity standpoint and that the plant can be operated at 100% power without impairment of public health and safety.

REFERENCES

1. Letter dated September 15, 1987, from W. L. Stewart, VEPCO, to Director of Nuclear Reactor Regulation, NRC, Accession No. 8709160239.

2. VEPCO Report, "North Anna Unit 1 July 15, 1987, Steam Generator Tube Rupture Event Report," September 15, 1987, Revision 1. (This report is docketed as part of Reference 1 above.)

3. Westinghouse Report WCAP-11601 (Proprietary Version) and WCAP-11602 (Non-Proprietary Version), "North Anna Unit 1 Steam Generator Tube Rupture and Remedial Actions Technical Evaluation," September 1987. NRC Accession Nos. 8710050087 and 8710050084.

4. NRC Augmented Inspection Team (AIT) Report Nos. 50-338/87-24 and 50-339/87-24, Inspection Conducted July 15-August 14, 1987, NRC Accession No. 8709040277.

5. USNRC Inspection Report No. 50-338/87-28, August 10-14, 1987, NRC Accession No. 8709090321.

6. USNRC Inspection Report No. 50-338/87-31, August 31-September 4, 1987.

7. Bates, R. C. and Clark, W. G., Jr., Transactions of the American Society for Metals, Vol. 62, 1969, p. 380.

8. Westinghouse presentation to NRC staff and VEPCC on August 17, 1987, at Westinghouse Research Center, Pittsburgh.

9. NRC consultant's report authored by R. G. Ballinger, "North Anna #1, Steam Generator, Row 9, Column 51 Tube Failure Analysis," October 19, 1987.

10. [

11.

]

12. Westinghouse letter NS-NRC-87-3285, dated November 2, 1987, to NRC, "Slide Presentation Material of November 4, 1987" (Proprietary Information).